Stress Analysis and Optimization of Hot-Formed Lightweight Wheels

B. Li, M. T. Ma(✉), P. Zhou, and J. W. Li

Zhongxin (Chongqing) Ultra High Strength Material Research Institute Co., Ltd., Chongqing, China

mingtuma@126.com

Abstract. The configuration of the 22.5 × 9.00 hot-stamped lightweight wheel was optimized based on finite element stress analysis in this article. To reach the goal of reducing working stress and meeting the experimental requirements along with the experimental enhancement coefficient, under the optimized condition for the wheel weight being 28 kg, the finite element stress analysis was carried out on the following three optimizations: increasing the spoke's thickness, modifying the shape and size of the windows, and setting up 3 mm-depth recessed structures between the windows. With the experimental enhancement coefficient of the bending fatigue test as 1.1 and the experimental enhancement coefficient of the radial loading fatigue test as 1.6, the numerical simulation results showed that the wheel's stress under bending and radial loading conditions decreased by 35.9% and 26.83% respectively after configuration optimization, which successfully achieved the requirements of the 28 kg lightweight wheel.

Keywords: Lightweight wheel · Hot-formed · Stress analysis

1 Introduction

Generally, a commercial vehicle trailer needs at least 6 wheels, and a stake truck requires even more, over 12 wheels. As for a 22.5″ × 9″ wheel, the one made of 380CL steel weighs over 40 kg, and even the one made of high-strength steel weighs around 36 kg. On the grounds that wheels are rotating parts belong to unsprung mass and account for a big proportion of a vehicle's total weight, their weight reduction is significantly crucial for automotive lightweighting.

Wheels, rotating parts, bear fatigue loading and are critical safety components. Their function directly affects the safety, reliability, and comfort of the vehicle. Therefore, their performance after weight reduction needs to meet higher requirements. As the wheel structure of commercial vehicles is complex, it is hard to resolve springback problems by using high-strength steel for weight reduction. However, hot-stamping can solve these problems and produce ultra-high-strength steel parts, which is an effective strategy for automotive lightweighting. To make the best use of hot-stamping, the configuration optimization of the wheel was conducted first.

Y. Zhang and M. Ma (Eds.): ICHSU 2022, AHMST 2, pp. 355–362, 2023.
https://doi.org/10.2991/978-94-6463-114-2_47

(a) (b)

Fig. 1. The layout (a) and numerical model (b) of the wheel.

In this paper, a lightweight wheel of a 28 kg target weight was designed in accordance with standards [1] and [2] for the wheel design and experiment requirements. Steel with a tensile strength of 1500 MPa was adopted for the hot stamping process. Considering the failure modes and the loads of 3750 kg, the stress analysis was carried out on the optimized wheel. The numerical simulation was set up in Abaqus according to the function and experimental requirements of commercial vehicle wheels. The finite element stress analysis was conducted on the designed $22.5'' \times 9''$ hot-formed lightweight wheel under bending and radial loads to enhance the function of the lightweight wheel and its reliability.

2 The Hot-Stamped Lightweight Wheel

The hot-stamped wheel adopts steel with a yield stress of 1200 MPa and tensile strength of 1500 MPa. The windows on the disc are designed as ellipses. The layout and the numerical model of the wheel are shown in Fig. 1. The model weighs 28.18 kg.

3 The Stress Analysis of the Wheel Before Optimization Under Bending and Radial Loads

3.1 Loads and Boundary Conditions for Stress Analysis

The schematic diagram of the bending fatigue test, the finite element model, loads, and boundary conditions are shown in Fig. 2 and 3. The rated load of the wheel was 3750 kg, and the bolt torque was 600 N·m. The disc and the rim were meshed with second-order 10-node tetrahedron elements (C3D10). As shown in Fig. 3, all translations and rotations at the edge of the rim were fixed. A concentrated force was applied on the drive shaft vertically.

According to standard [2], the bending moment was calculated by the following formula:

$$M = (\mu R + d)FvS \tag{1}$$

where,

$\mu = 0.7$, coefficient of friction between tires and roads

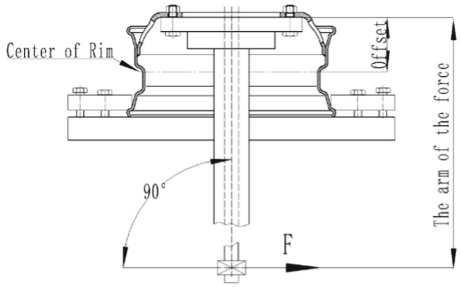

Fig. 2. Schematic diagram of the bending fatigue test.

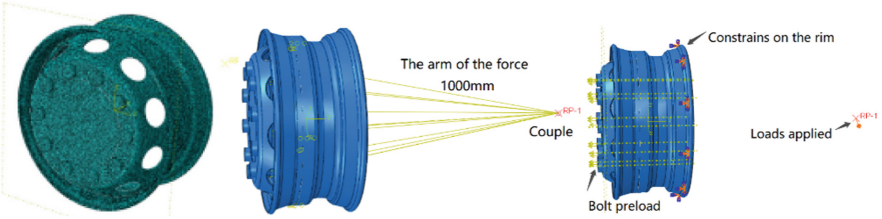

Fig. 3. Loads and boundary conditions of the finite element model.

$R = 504$ mm, the radius of the biggest tire can be installed on the wheel under static loads

$d = 175$ mm, wheel offset

$Fv = 37500$ N, rated load of the wheel (Gravitational acceleration is made to be 10 m/s^2 to simplify calculation.)

$S = 1.1$, experimental enhancement coefficient

$M =$ Bending moment

Calculation results:

$M = 21771$ N·m

As $M = F \times L$,

where,

F is bending load

$L = 1$ m, the arm of the force

Thus, $F = M/L = 21771$ N

The schematic diagram of the radial loading fatigue test and the finite element model are shown in Fig. 4. The rated load of the wheel was 3750 kg, and the spoke and the rim were meshed with the second-order 10-node tetrahedron elements (C3D10). In the dynamic radial fatigue test, the steel rim also bore bolt preload, gravity, and centrifugal force during high-speed rotation, but these forces were ignored as their influence on the simulation results was insignificant [4]. The boundary conditions and loads applied are shown in Fig. 4(b).

According to standard [2], the radial load was calculated by the following formula:

$$Fr = FvK \tag{2}$$

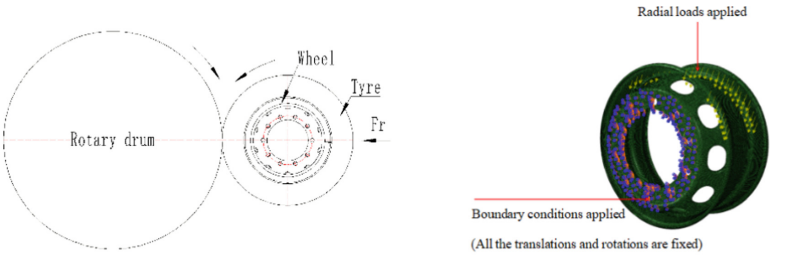

Fig. 4. Schematic diagram of radial loading fatigue test (a) and finite element model (b).

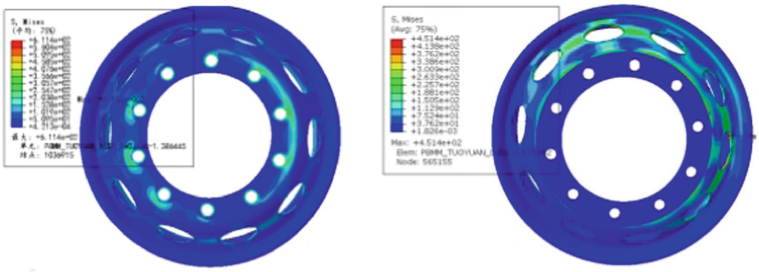

Fig. 5. Stress distribution of the wheel under bending loads (a) and radial loads (b).

where,

Fr = radial load.

Fv = 37500 N, rated load of the wheel (Gravitational acceleration is made to be 10 m/s^2 to simplify calculation.)

K = 1.6, experimental enhancement coefficient.

Calculation results:

Fr = 60000 N.

3.2 The Numerical Simulation Results

Based on the finite element modeling methods described in part 1) and 2) of 3.1 section the stress distribution of the wheel under bending loads is shown in Fig. 5(a). The maximum stress is 611.4 MPa, around the bolt holes. The stress distribution of the wheel under radial loads is shown in Fig. 5(b). The maximum stress is 451.4 MPa, which is located at the windows on the spoke.

4 Optimization for Stress Improvement

4.1 Increasing the Thickness of the Spoke

The thickness of the spoke was optimized from 8 mm to 8.5 mm. The numerical simulation results are shown in Fig. 6. The maximum stress under the bending loads around the bolt holes is 578.2 MPa shown in Fig. 6(a), decreasing by 33.2 MPa.

4.2 Optimization the Configuration of the Windows

The shape and size of the windows will affect both the weight of the wheel and the stress distribution. To obtain an ideal lightweighting result and ensure that the windows bear forces equally, the number of the windows and bolt holes should be the same. In this paper, the most common design, a 10-window wheel, was adopted, and the windows' original shape was an ellipse, as shown in Fig. 7. To further reduce weight after the increase in the disc's thickness to 8.5 mm, the elliptic windows were optimized to oblong windows with a larger area, as shown in Fig. 8. After the optimization, the wheel weight decreased by 0.14 kg, and the area of the window increased by 3000 mm^2. This new design not only increased the area of the window to improve the ventilation but also reduced the wheel weight. The stress analysis results before optimization are shown in Fig. 6, and the stress analysis results after optimization are shown in Fig. 9. After optimization, the maximum stress under bending loads is 541.2 MPa, located at the bolt holes, decreasing by 37 MPa. The maximum stress under radial loads is 396.3 MPa, located in the windows, decreasing by 47.6 MPa. Thus, the optimization is effective.

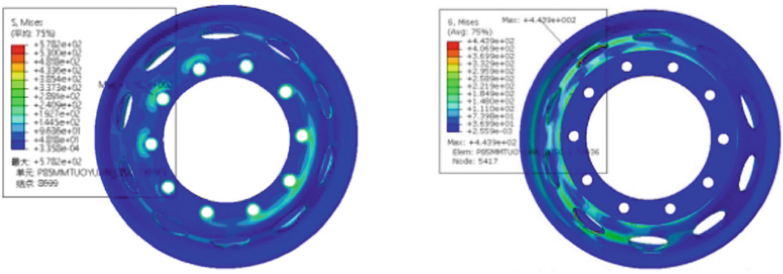

(a) (b)

Fig. 6. Von-mises stress plot under bending loads (a) and Von-mises stress plot under radial loads (b).

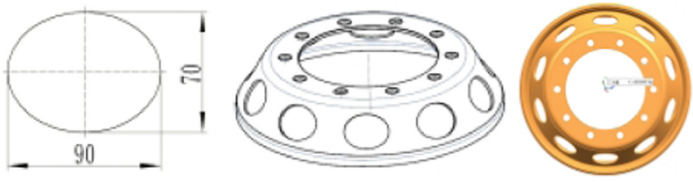

Fig. 7. Elliptic windows.

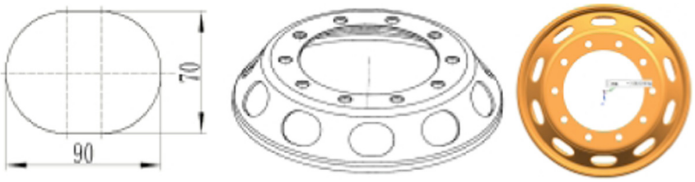

Fig. 8. Oblong windows.

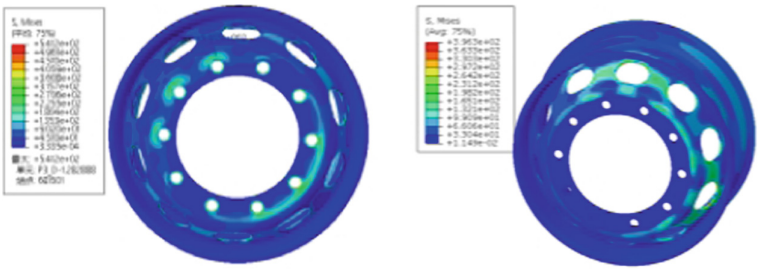

(a) (b)

Fig. 9. Von-mises stress plot under bending loads (a) and von-mises stress plot under radial loads (b) after optimization.

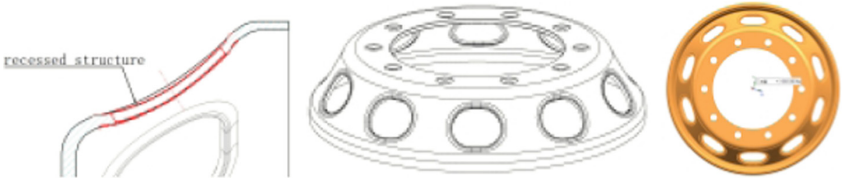

Fig. 10. Optimized design and model.

4.3 Optimization of the Surface Structure of the Disc

As the sharp edges and burrs on the windows of the wheel after punching cannot be entirely cleared after treatment, the disc is prone to cracking. To further improve the deformation resistance of the windows, a 3 mm-depth recessed structure was set up for each window. The optimized design and numerical simulation results are shown in Fig. 10 and Fig. 11. After optimization, the maximum stress at the windows under the bending loads is 194.4 MPa, which is 38.6 MPa lower than that before optimization (233 MPa). Besides, the maximum stress is located at the bolt holes and decreases to 511.2 MPa, which is 30 MPa lower than that before optimization. As for the maximum stress under radial loads, it is in the windows and decreases to 340.2 MPa, which is 56.1 MPa lower than that before optimization. Hence, the optimization effectively reduced the stress at the windows under bending and radial loads and brought down the possibility of crack initiation (Fig. 12).

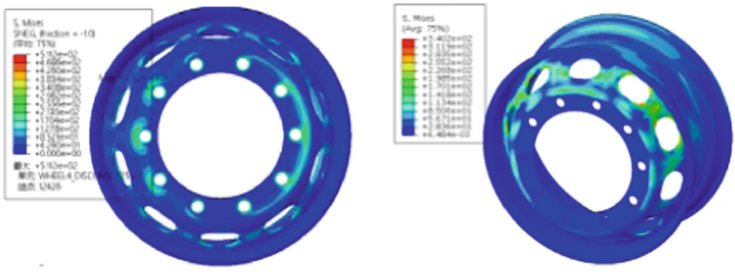

(a) (b)

Fig. 11. Von-mises stress plot under bending loads (a) and von-mises stress plot under radial loads (b) of the optimized design.

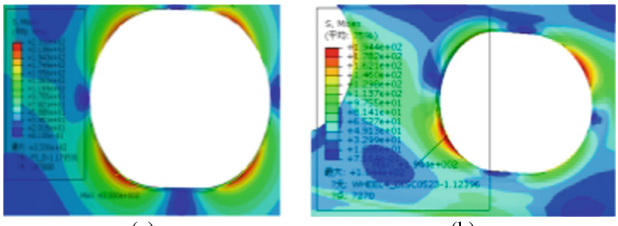

(a) (b)

Fig. 12. Stress distributions of the windows under bending loads before (a) & after (b) optimization.

5 Conclusion

As the numerical simulation results showed, the stress of the wheel was effectively reduced after optimization. Due to the partial thinning of wheel parts in the process of stamping and spinning, the weight of the redesigned 22.5″ × 9.00″ hot-stamped lightweight wheel was expected to be less than 28 kg according to experience estimate from numerical model, which achieved the goal of weight reduction. Moreover, the stresses are decreased due to optimization design which improved the wheel's reliability in the using.

Acknowledgments. The work is supported by grant 2-4570.5 of the Swiss National Science Foundation.

References

1. Rims for truck-bus: GB/T 31961-2015, Beijing: Standards Press of China, (2016).
2. Performance Requirements and Test Methods of Commercial Vehicles Wheels: GB/T5909–2009, Beijing: Standards Press of China, (2010).

3. X. Zhu, Analysis of lightweight design of light commercial vehicles, *Shanghai Automobile* **10**, 29 (2015).
4. S. X. Han, Simulation and research on performance of steel wheel, *Auto Time* **7**, 110 (2018).